

Identification, Characterization, and Site-Specific Mutagenesis of a Thermostable ω -Transaminase from *Chloroflexi bacterium*

Chen Wang, Kexin Tang, Ya Dai, Honghua Jia,* Yan Li,* Zhen Gao, and Bin Wu

Cite This: *ACS Omega* 2021, 6, 17058–17070

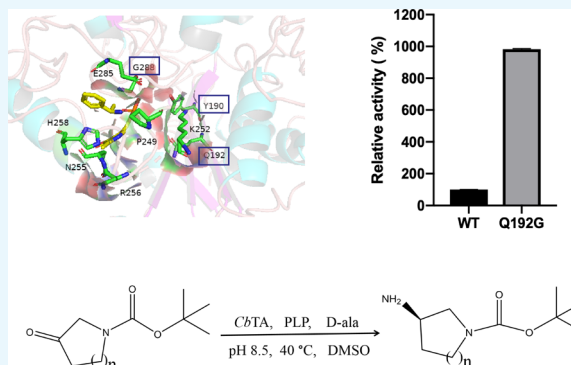
Read Online

ACCESS |

Metrics & More

Article Recommendations

ABSTRACT: In the present study, we have identified an ω -transaminase (ω -TA) from *Chloroflexi bacterium* from the genome database by using two ω -TA sequences (ATA117 Arrmut11 from *Arthrobacter sp.* KNK168 and amine transaminase from *Aspergillus terreus* NIH2624) as templates in a BLASTP search and motif sequence alignment. The protein sequence of the ω -TA from *C. bacterium* (*CbTA*) shows 38% sequence identity to that of ATA117 Arrmut11. The gene sequence of *CbTA* was inserted into pRSF-Duet1 and functionally expressed in *Escherichia coli* BL21(DE3). The results showed that the recombinant *CbTA* has a specific activity of 1.19 U/mg for (*R*)- α -methylbenzylamine [(*R*)-MBA] at pH 8.5 and 45 °C. The substrate acceptability test showed that *CbTA* has significant reactivity to aromatic amino donors and amino receptors. More importantly, *CbTA* also exhibited good affinity toward some cyclic substrates. The homology model of *CbTA* was built by Discovery Studio, and docking was performed to describe the relative activity toward some substrates. *CbTA* evolved by site-specific mutagenesis and found that the Q192G mutant increased the activity to (*R*)-MBA by around 9.8-fold. The Q192G mutant was then used to convert two cyclic ketones, *N*-Boc-3-pyrrolidinone and *N*-Boc-3-piperidone, and both the conversions were obviously improved compared to that of the parental *CbTA*.



1. INTRODUCTION

Chiral amines are very important intermediates, which have a wide range of applications in medicine and fine chemical industries.¹ The production of chiral amines includes chemical and biochemical methods. As far as chemical methods are concerned, chiral amines are usually produced by the asymmetric catalysis of prochiral molecules, such as hydrogenation of imine or enamine, alkylation of imine, amino hydroxylation, and reductive amination.² In order to overcome the drawbacks of low enantioselectivity, need for noble-metal catalysts, harsh reaction conditions, and environmental concerns in asymmetric synthesis, several biochemical methods using efficient biocatalysts have been developed and managed to replace chemical methods. These methods mainly involve enzymes such as amine oxidases, ammonia lyases, amine dehydrogenases, and transaminases.^{3–5} Among them, ω -transaminases (ω -TAs), which catalyze the transfer of ketone and amino groups, have received extensive attention.^{6–9} The well-known example of the synthesis of chiral amines by ω -TAs is the manufacturing of sitagliptin, an oral antihyperglycemic drug.¹⁰

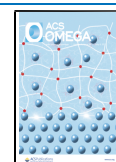
Interestingly, ω -TAs originating from various sources have shown distinct enantioselectivity, that is, (*R*)-selective or (*S*)-selective. Hence, both enantiomers of specific amines can be produced by ω -TAs with different enantioselectivities. Although the ω -TA Ata-117 Arrmut11 from *Arthrobacter sp.* KNK168 is

commercially available now, only a few (*R*)-selective ω -TAs have been identified.^{11,12} Therefore, the discovery of novel *R*-selective ω -TAs has still been the focus issue in the past few years. Bornscheuer et al.^{13,14} developed a method for predicting and screening enzyme functions on the basis of a key motif in sequence, which has been proved to be effective and successfully used to search and identify 17 (*R*)-selective ω -TAs by database mining. The method has also been applied to discover five other different sources of (*R*)-selective ω -TAs.¹⁵ In recent years, more and more (*R*)-selective ω -TAs have been discerned and investigated, but their wide applications are still limited by their poor properties.^{16–18} In order to improve the performance of enzymes, protein engineering has usually been adopted to conduct enzyme design and optimization. An (*R*)-selective ω -TA has been created by bioinformatic analysis combined with the computational redesign of the D-amino acid amino-transferase, exhibiting a specific activity close to those of natural

Received: April 23, 2021

Accepted: June 3, 2021

Published: June 25, 2021



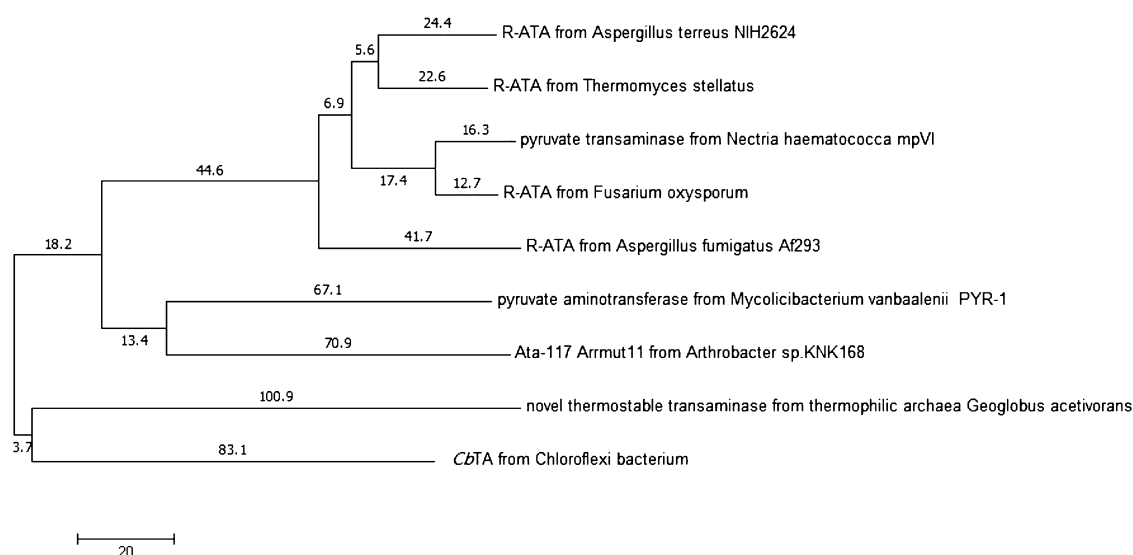


Figure 1. Phylogenetic analysis of *CbTA* from *C. bacterium* and related proteins. The phylogenetic tree was constructed using the neighbor-joining algorithm in the molecular evolutionary genetic analysis package (MEGA 7) and the relative positions of the proteins were highlighted and labeled with species names.

(*R*)-selective ω -TAs.¹⁹ On the basis of a fluorescence-based screening system, a KnowVolution campaign has been carried out to optimize a (*R*)-selective ω -TA from *Mycobacterium vanbaalenii*, and the best resulting mutant showed specific activity to acetonaphthone more than 100 times higher than that of the parental enzyme.²⁰ In another study, a (*R*)-selective ω -TA from *Arthrobacter cummingsii* ZJUT212 has been modified using a semirational protein design, and a mutant has been screened to produce the sitagliptin intermediate on a kilogram scale with >99% e.e. and approximately 80% conversion.²¹

In the current study, BLAST search (<https://blast.ncbi.nlm.nih.gov/Blast.cgi>) was performed against an NCBI non-redundant protein sequence library to identify a putative ω -TA sequence from *Chloroflexi bacterium* (*CbTA*) using Ata-117 Arrmut11 from *Arthrobacter sp.* KNK168 and amine transaminase from *Aspergillus terreus* NIH2624 as templates. Subsequently, the gene of *CbTA* was cloned into *Escherichia coli* for expression, and its kinetic parameters and substrate spectra were characterized. Thereafter, *CbTA* was improved by site-specific mutagenesis on the basis of the reported results and modeling analysis.

2. RESULTS AND DISCUSSION

2.1. Sequence Analysis. Nowadays, more and more protein sequences are stored in the database, which provides a huge resource for the mining of biocatalysts. Ata-117 Arrmut11 from *Arthrobacter sp.* KNK168 (PDB ID: 5FR9), a variant of the KNK168 with mutations in 27 positions with excellent stereoselectivity, has been successfully applied to industrial synthesis and a series of kinetic resolution.^{10,22} The amine transaminase from *A. terreus* NIH2624 (PDB ID: 4CE5) is another important template used to explore the functional motif of (*R*)-selective ω -TAs and has been shown to be highly active.¹⁴ Two independent BLAST searches were performed using two crystallized (*R*)-selective ω -TAs, Ata-117 Arrmut11 from *Arthrobacter sp.* KNK168 and amine transaminase from *A. terreus* NIH2624 as templates. Then, rational analysis of the aligned sequences was performed using a motif sequence alignment, following the criteria previously established by Hühne and Bornscheuer.¹⁴ Four putative sequences derived

from thermophilic bacteria were obtained from the NCBI nonredundant protein sequence library: EAYS7657.1 (*Leptospirillum rubarum*), EES52356.1 (*Leptospirillum ferrodiazotrophum*), RIK47101.1 (*Chloroflexi bacterium*), and RLT41415.1 (*Chloroflexi bacterium*). The construction and expression of the four enzymes are the same. According to the preliminary activity test, the crude enzyme activities of these four enzymes were 0.207, 0.124, 0.91, and 0.248 U/mg, respectively. Among them, *CbTA*, the ω -TA from *C. bacterium* (RIK47101.1) with the highest activity, was selected as the target for further study.

CbTA showed identity with amine transaminases from the following microorganisms: *Arthrobacter sp.* KNK168²³ (PDB ID: 3WWH; 38%), *A. terreus* NIH2624²⁴ (PDB ID: 4CE5; 36.1%) *Aspergillus fumigatus* Af293²⁵ (GenBank accession no. EAL86783; 37.2%), *Archaeoglobus fulgidus* DSM 4304²⁶ (PDB ID: 5MQZ; 37.8%), *Nectria haematococca* MPVI²⁷ (PDB: 4CMD; 36.8%), *M. vanbaalenii* PYR-1 (GenBank accession no. ABM15291; 35.9%), and *Geoglobus acetivorans*²⁶ (PDB ID: 5E25; 35.8%). Although the identity with the reported sequence is not high, the functional sites of R86, K188, and E221 are conservative after alignment. Phylogenetic tree analysis is performed to verify the taxonomic and evolutionary relationship of *CbTA* to previously reported transaminases, and the results are presented in Figure 1. Nine amino acid sequences with different degrees of sequence identity to *CbTA* were collected and compared. *CbTA* was found to have a close evolutionary relationship with thermophilic archaea *Geoglobus acetivorans*.

2.2. Purification and Identification of the Recombinant *CbTA*. The recombinant *E. coli* BL21(DE3)/pRSF-*CbTA* cells were cultured, collected, and sonicated. The expressed recombinant protein with a theoretical molecular weight of 44.3 kDa and was detectable in the soluble part of *E. coli* BL21 (DE3)/pRSF-*CbTA* cells (Figure 2). The recombinant protein is purified by immobilized metal ion affinity chromatography with the assistance of His-tag at the *N*-terminus of the sequence, and the purification results are shown in Figure 2. The followed activity test indicated that the specific activity of *CbTA* to (*R*)- α -methylbenzylamine [(*R*)-MBA] was 1.19 U/mg at pH 8.5, 45 °C.

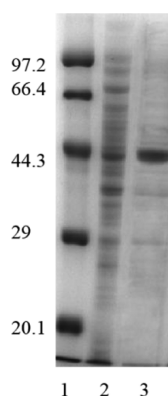


Figure 2. SDS-PAGE of *CbTA*. Lane 1, protein markers; lane 2, crude extract; and lane 3, purified enzyme.

2.3. Enzymatic Properties of *CbTA*. As shown in Figure 3a, the effect of pH on *CbTA* activity is assessed over the range of pH 6.0 to 10.5, and *CbTA* has the highest activity at pH 8.5, which is similar to the known ω -TAs.^{28,29} For example, a typical (*R*)-selective ω -TA from *Arthrobacter* sp. KNK168 has shown an

optimal pH of 8.0 to 9.0.³⁰ Besides, a branched-chain amino acid aminotransferase TUZN1299 identified from the genome of the hyperthermophilic archaeon *Thermoproteus uzoniensis* has exhibited an optimal pH of 8.0.³¹ The influence of temperature on *CbTA* activity was evaluated over a range of 25–65 °C, and the highest activity was detected at 45 °C (Figure 3b). Figure 3c presents the temperature profile of *CbTA*, and results show that it has good thermal stability. Interestingly, with the increase of incubation time at 45 °C, the highest activity of *CbTA* can reach twice of the original activity. The possible mechanisms for stability are high bulk density, optimal charge pattern or ion pair, and minimized hydrophobic surface area and helical stability.³² This increase in activity is probably caused by temperature-related folding that increases stabilizing interactions, thus improving its reactivity; we also noticed a similar increase in an thermophilic transaminase from *Geobacillus thermodeliniifcans*.³³ The temperature dependence also showed that *CbTA* retains 50% activity after 12 h of incubation at 50–55 °C, but it was significantly inactivated at above 60 °C. Similarly, most of the thermophilic TAs have shown significant thermal stability at about 55 °C.³⁴ For instance, it has been found that a transaminase identified from *Thermomicrobium roseum* retained

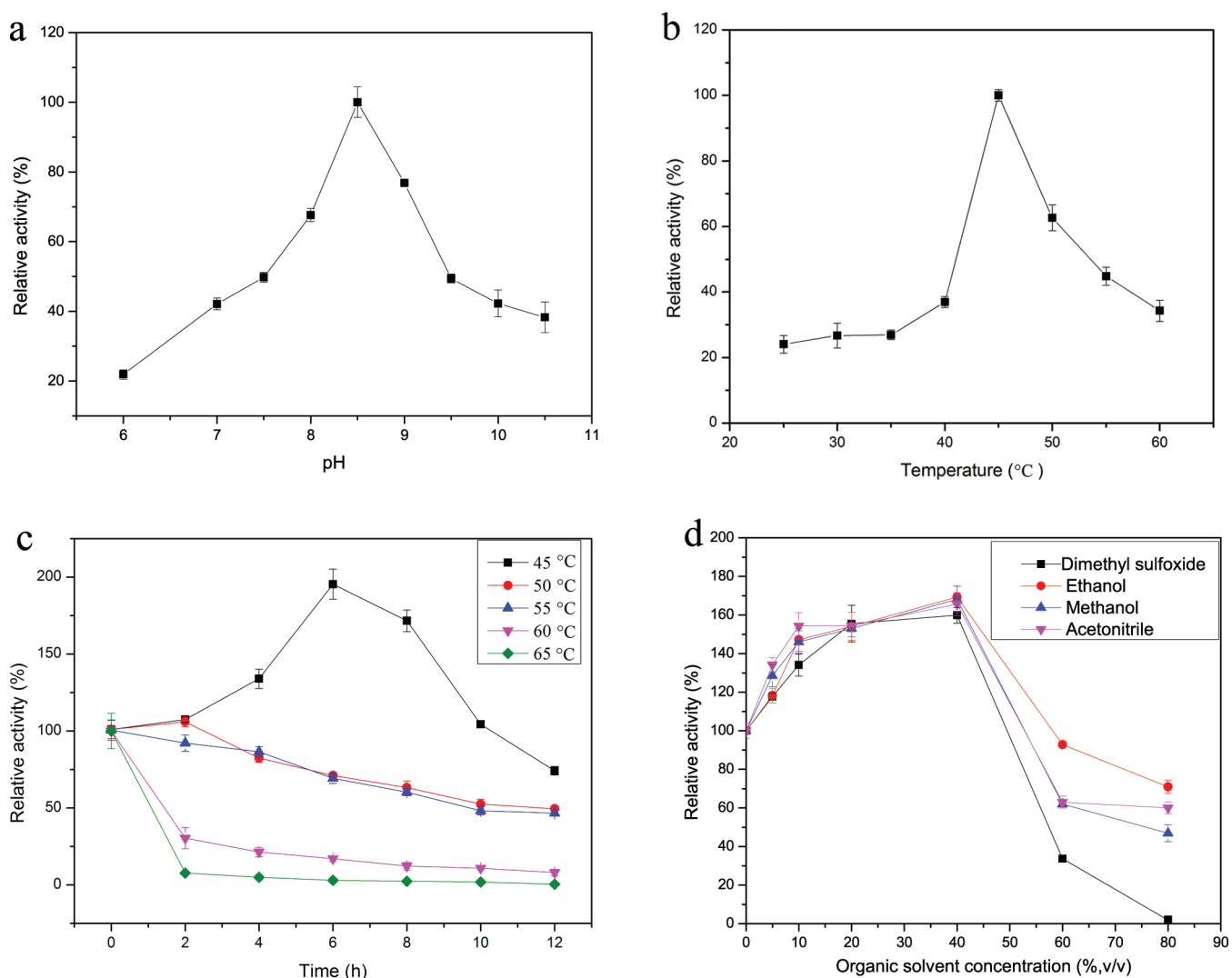


Figure 3. Characterization of enzymatic properties of *CbTA*. (a) Optimum pH; (b) optimum temperature; (c) temperature stability; and (d) effect of organic cosolvent concentration on *CbTA* activity.

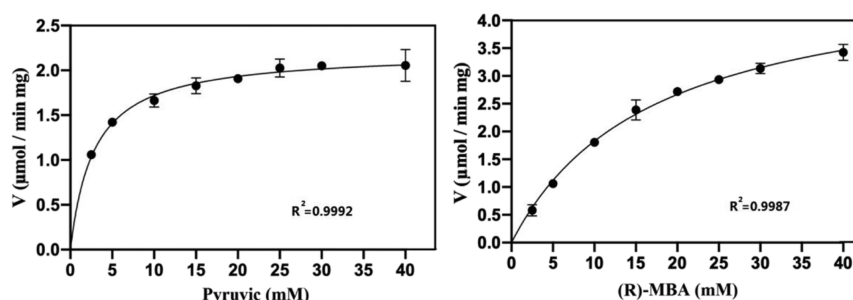
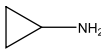
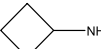
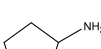
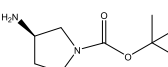
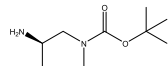


Figure 4. Nonlinear regression fitting of the Michaelis–Menten equation.

Table 1. Amino Donor Specificity of *CbTA* for Aliphatic and Aromatic Amines

Amino donor	R1	R2	Relative activity (%) ^a
A1	–C ₆ H ₅	–CH ₃	100
A2	–CH ₃ CH ₂	–H	66
A3	–CH ₃	–CH ₃	<1
A4	–CH ₂ CH ₃	–CH ₃	nd
A5	–(CH ₂) ₂ (CH ₃) ₂	–H	50
A6	–CH ₂ CH ₃	–CH ₂ CH ₃	38
A7	–(CH ₂) ₄ CH ₃	–CH ₃	67
A8	–(CH ₂) ₅ CH ₃	–CH ₃	109
A9			60
A10			61
A11			74
A12			35
A13			85
A14	–C ₆ H ₅	–H	<1
A15	–CH ₂ C ₆ H ₅	–H	42
A16	–CH ₂ C ₆ H ₅ (4-OH)	–H	76
A17	–C ₆ H ₄ (3-Cl)	–CH ₃	115
A18	–(CH ₂) ₂ C ₆ H ₅	–CH ₃	82

^aReaction conditions in Tables 1 and 2: 0.1 mg mL^{−1} purified enzyme, 25 mM pyruvate and 25 mM amino donor, 1 mL of glycine–NaOH buffer (50 mM, pH 8.5), and 40 °C. One unit of enzyme activity was defined as the conversion of 1 μmol pyruvate per minute. The relative activity for (R)-MBA was designated as 100%.

50% activity after 5 h of incubation at 70 °C.³⁵ A β-amino acid transaminase Ms-TA2, which has been discovered in the genome of the *Meiothermus* strain isolated in an Icelandic hot spring, kept around 60% activity after incubation at 50 °C for 3 h.³⁶ However, few thermophilic TAs remain active after incubation at temperatures above 65 °C. A novel amine transaminase has demonstrated spectacular thermostability, and its activity can be maintained at 85% or around 40% after being incubated at 80 °C for 5 or 14 days.³⁷

The organic cosolvent is very necessary to increase the solubility of substrates. The influence of the organic cosolvent on *CbTA* activity was determined by adding methanol, ethanol, dimethyl sulfoxide (DMSO), and acetonitrile in reaction solutions (Figure 3d). Results showed that the activity of *CbTA* increased significantly in all four 20–40% organic cosolvents, while it decreased in 60% organic cosolvents. This indicates that *CbTA* is well tolerable to the organic solvents and the results are superior to that of a solvent-tolerant haloarchaeal

(R)-selective transaminase isolated from a Triassic Period salt mine.³⁸

2.4. Kinetic Parameters of CbTA. The kinetic parameters are helpful to evaluate the catalytic ability of enzymes. Given that transaminases operate via a typical dual substrate recognition, the K_m and k_{cat} to either substrate of CbTA were determined by changing the concentration of (R)-MBA or pyruvate from 2.5 to 40 mM, respectively. With 20 mM pyruvate as a cosubstrate, the K_m and k_{cat} of CbTA to (R)-MBA are 14.68 mM and 3397.63 s⁻¹, while the K_m and k_{cat} of CbTA for pyruvate are 2.834 mM and 1617.5 s⁻¹, respectively. Compared with the ATA117 from *Arthrobacter sp.* KNK168, CbTA showed similar affinity for pyruvate, but its K_m value for (R)-MBA was significantly higher than that of ATA117, which indicated that CbTA had a slightly lower affinity for amine. However, CbTA showed lower K_m to pyruvate and higher k_{cat} than a transaminase from *Fusarium oxysporum*,³⁹ which means higher reactivity on pyruvate (Figure 4).

2.5. Substrate Specificity of CbTA. Previous studies on the substrate range and stereoselectivity have shown that the active center of transaminase is composed of two active pockets. The large pocket can embrace the large group and the small pocket is usually limited to methyl-sized substituents.⁴⁰ Considering the binding of the substrate to the ω -TA active center, we resolved the structure of the substrate on the basis of the ω -TA active site model, and the ω -TA's large pocket embraces R1, while the ω -TA's small pocket contains R2. All substrates were divided into four groups as follows: aromatic and aliphatic amines, amino acids, ketones, and aldehydes to allow us to compare reactivity chemically.

As shown in Tables 1–4, we can find that CbTA can utilize a wide range of amino donors and acceptors for the substrate

Table 2. Amino Donor Specificity of CbTA for Amino Acids

amino donor	R1	R2	relative activity (%) ^a
B1	-(CH ₂) ₂ COOH	-COOH	36
B2	-(CH ₂) ₃ NHNH ₂ NH	-COOH	38
B3	-CH ₂ SH	-COOH	48
B4	-CH ₂ COOH	-CH ₃	4

^aReaction conditions in Tables 1 and 2: 0.1 mg mL⁻¹ purified enzyme, 25 mM pyruvate and 25 mM amino donor, 1 mL of glycine–NaOH buffer (50 mM, pH 8.5), and 40 °C. One unit of enzyme activity was defined as the conversion of 1 μ mol pyruvate per minute. The relative activity for (R)-MBA was designated as 100%.

range, which is consistent with the literature⁴¹, indicating their potential for synthetic applications. It can be seen from Table 1 that CbTA has good activity for most aliphatic and aromatic amines, but there is a marked difference among the various aliphatic or aromatic amines, which is similar to the results reported by Jiang et al.¹⁵ A comparison of the relative activity of CbTA to aliphatic amines revealed that it showed a higher activity for the long-chain amines (A5–A8), while it exhibited a very low reactivity against the short-chain amines, isopropylamine (A3) and 2-butylamine (A4), except for propylamine (A2). Interestingly, CbTA displayed higher reactivity to propylamine but extremely low to isopropylamine unlike other amine transaminases. Furthermore, CbTA is quite reactive to cyclic amines, and its relative activity is normally better with the increase of the ring (A9–A13). Unexpectedly, when amino acids are used as the amino donors (B1–B4), the activity given by

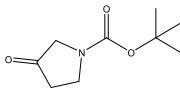
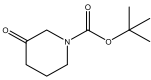
CbTA is not very high, or even very low, for example, 2-aminobutyric acid (B5).

The amino receptor specificity of CbTA is studied and the results are presented in Tables 3 and 4. CbTA appears to have similar amino receptor specificity for *Capronia semiimmersa*.⁴² The amino receptor spectrum shows that CbTA has low reactivity to nearly all aliphatic, cyclic, and aromatic ketones except for 2'-nitroacetophenone (C7), 4'-methoxyacetophenone (C8), benzaldehyde (D5), and 5-nitrosalicylaldehyde (D6). According to the results given in tables, amino acceptors with an aryl group have comparatively good reactivity for CbTA, and aryl ketones and aromatic aldehydes present similar results. However, low activity for CbTA is observed in the case where the selected aliphatic ketones or aldehydes were used as amino acceptors. In comparison, the reactivity of CbTA toward aliphatic ketones and aldehydes was different from previously reported results.⁴³ It should be noted that in most cases benzene ring with methyl substituent group in aryl ketones would dramatically inhibit the reactivity of amino acceptors, and the existence of methylene between aryl group and aldehyde group also significantly reduced the activity of CbTA to aryl aldehydes. Additionally, CbTA appears to be reactive to two selected cyclic substrates with ketone groups.

Discovery studio proposed an active site model of CbTA binding to pyridoxal 5'-phosphate (PLP). The most favorable binding model contains several reported key residues. Previous study has reported that residue K252 shows significant catalytic reactivity with coenzymes and substrates.⁴⁴ As is shown in Figure 5, K252, which binds to the center of the pocket, has a strong hydrogen bond force and attractive charge with PLP. At the same time, a strong hydrogen bond force was also found between PLP and residues G288 and S346. Residue E285 is located in the substrate-cofactor binding pocket and has a conventional hydrogen bonding with the amino group of (R)-MBA. In addition, it is observed that the force contribution of the oxygen atom of the phosphate group in PLP was provided by K252, G288, and E285, which is similar to other (R)-selective transaminase.⁴⁵

To manage to explain the possible cause of substrate specificity, some selected amino donors and acceptors were docked with CbTA and PLP, and the results were visualized by Discovery Studio (Figure 6 and Figure 7). The most favorable docking configuration was selected to analyze the forces. As is shown in Figure 6, from the docking results of aliphatic amines (A2–A8), residues in binding sphere of CbTA might have π -alkyl and attractive charge on the carbon chain, except isopropylamine (A3), which explains the low reactivity for A3. According to the docking results of cyclic amines, PLP has strong acting forces, such as π -cation interaction and conventional hydrogen bond, on the amino groups of cyclic substrates cyclobutanamine (A10) and cyclopentylamine (A11), while the acting force on amino groups of cyclopropylamine (A9) is only the C–H bond. It seems that with the increase of the size of the cyclic substrate, the L-pocket becomes more suitable for binding ligands. When aromatic substrates were involved, there were many intermolecular forces between residues in binding sphere and benzene ring, including T-shaped π - π stack and π -alkyl interactions. Taking (R)-1-(3-chlorophenyl) ethylamine (A17) as an example, we could see that residues R287 and Q259 have a strong conventional hydrogen bond with the amino group of A17 and that the chloro group in benzene ring is an electron-withdrawing group forming a π -alkyl force with residue H260, which may lead to high

Table 3. Amino Acceptor Specificity of *CbTA* for Keto Acids and Ketones

Amino acceptor	R1	R2	Relative activity (%) ^b
C1	-COOH	-CH ₃	100
C2	-CH ₂ CH ₃	-CH ₃	nd
C3	-CH ₂ CH ₃	-CH ₂ CH ₃	nd
C4			2.4
C5			14.7
C6	-(CH ₂) ₂ COOH	-COOH	nd
C7	-C ₆ H ₄ (2-NO ₂)	-CH ₃	238
C8	-C ₆ H ₄ (4-OCH ₃)	-CH ₃	259
C9	-C ₆ H ₄ (2-OH)	-CH ₃	21.8
C10	-C ₆ H ₄ (2-Br)	-CH ₃	<1
C11	-C ₆ H ₄ (2-F)	-CH ₃	2.9
C12	-C ₆ H ₄ (2-CH ₃)	-CH ₃	2.4
C13	-C ₆ H ₅	-CH ₂ OH	nd
C14	-C ₆ H ₅	-(CH ₂) ₃ CH ₃	nd
C15	-CH ₂ C ₆ H ₅	-CH ₂ C ₆ H ₅	6

^aReaction conditions in Tables 3 and 4: 0.1 mg mL⁻¹ purified enzyme, 25 mM (*R*)-MBA and 25 mM amino acceptor, 1 mL of glycine-NaOH buffer (50 mM, pH 8.5), and 40 °C. One unit of enzyme activity was defined as the conversion of 1 μmol acetophenone per minute. The relative activity for pyruvate was designated as 100%.

Table 4. Amino Acceptor Specificity of *CbTA* for Aldehydes

amino acceptor	R1	R2	relative activity (%) ^a
D1	-CH ₂ CH ₃	-H	1.2
D2	-(CH ₂) ₂ CH ₃	-H	6
D3	-CH(CH ₃) ₂	-H	5.7
D4	-CH(CH ₂) ₄ (CH ₃) ₂	-H	5.8
D5	-C ₆ H ₅	-H	272
D6	-C ₆ H ₃ (2-OH) (5-NO ₂)	-H	250
D7	-CH ₂ C ₆ H ₅	-H	26

^aReaction conditions in Tables 3 and 4: 0.1 mg mL⁻¹ purified enzyme, 25 mM (*R*)-MBA and 25 mM amino acceptor, 1 mL of glycine-NaOH buffer (50 mM, pH 8.5) and 40 °C. One unit of enzyme activity was defined as the conversion of 1 μmol acetophenone per minute. The relative activity for pyruvate was designated as 100%.

reactivity of A17. In addition, the low activity of benzylamine (A14) is probably because of the fact that coenzyme PLP has no interaction with it, and residue E259 also has an unfavorable donor-donor to its amino group.

The docking results of selected amino acceptors with the active site model of *CbTA* binding to PLP are shown in Figure 7. We could observe that pyridoxamine 5'-phosphate (PMP) has a strong hydrogen bond with the aldehyde group in the typical acceptor pyruvate (C1), and residues T242, N253, and H258 also bear the corresponding hydrogen bond with the aldehyde group and carboxyl group; we infer that this leads to strong affinity for pyruvic acid. As for α-ketoglutarate (C6), the

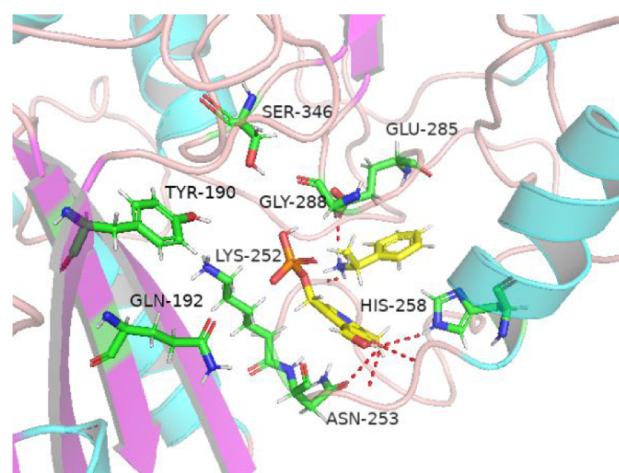


Figure 5. Model of the active site of *CbTA* binding with PLP and (*R*)-MBA. The key residues in the active site are shown in green.

interaction between PMP and the substrate was not found, which may be the reason why *CbTA* has no activity on C6. From the possible docking diagrams of ketones, it could be perceived that the active site of PMP and the enzyme tended to bind to stable structures containing benzene or rings and only exhibited weak van der Waals for straight chain substrates, which might be the reason why most of the aliphatic ketones were low or even inactive, for example, pentanone (C3). For the docking results of aromatic ketones, the electron-withdrawing groups of 2'-

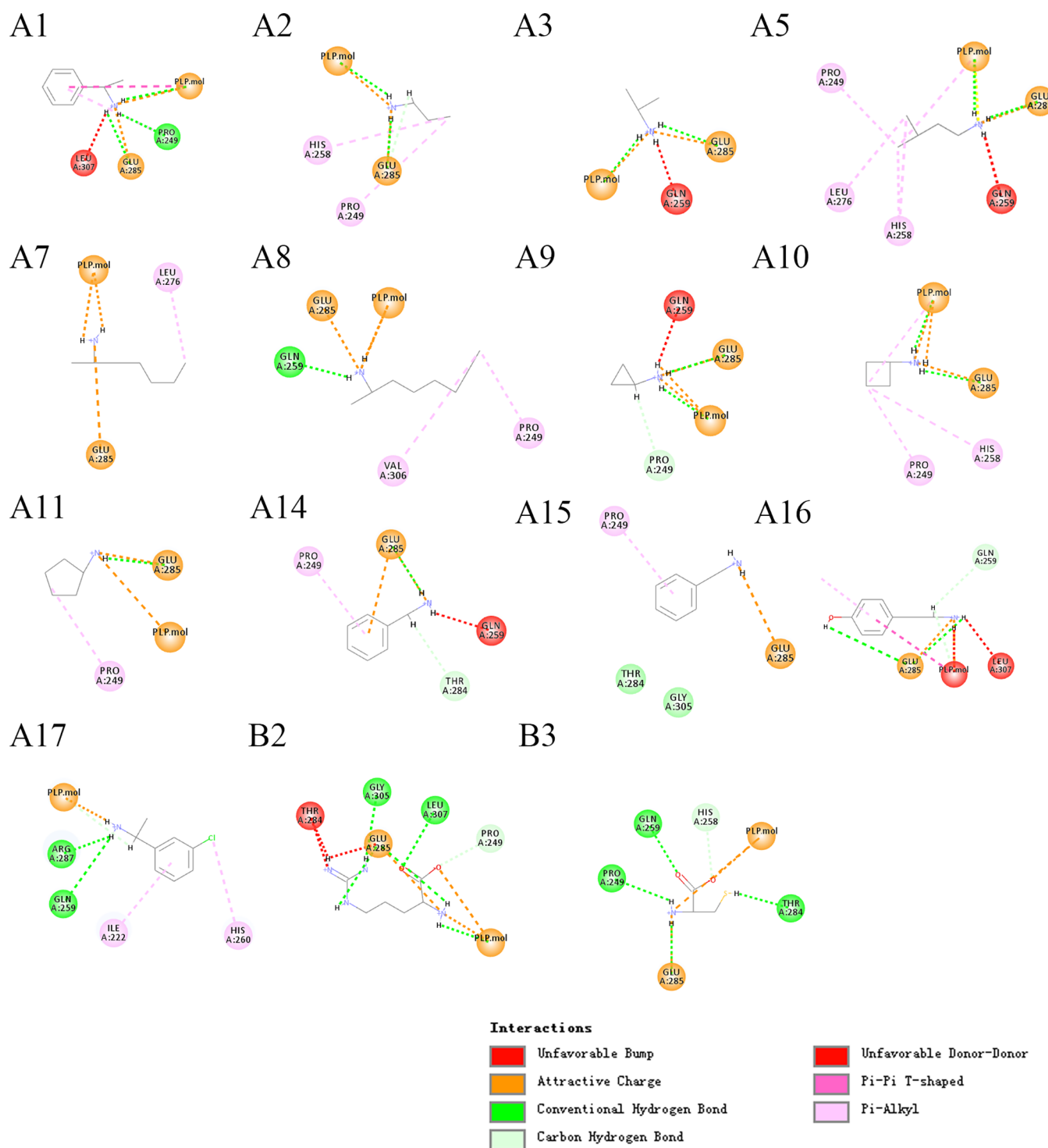


Figure 6. Docking results of *CbTA* with selected amino donors listed in Tables 1 and 2.

nitroacetophenone (C7) with good reactivity show the attractive charge and salt bridge with PMP. In the case of 4'-methoxyacetophenone (C8), PMP has a Pi-alkyl interaction with its benzene ring and other residues have a Pi-Pi T-shaped interaction and hydrogen bond with the benzene ring and ketone groups, with its methoxy group having an additional C-H interaction binding with *CbTA*. In contrast to other acceptors, the substituted R2 groups show little interaction with *CbTA* and PMP, suggesting that the small pocket of *CbTA* is not suitable for substrates with R2 more than one methyl group, which may

be responsible for the lack of activity of 2-hydroxyacetophenone (C13) and valerophenone (C14). For aldehydes, residues in both PMP and binding sphere have a conventional hydrogen bond with the aldehyde group except for propionaldehyde (D1) and 2-ethylhexanal (D4), which might explain the low reactivities of D1 and D4. With regard to the most reactive amino acceptors benzaldehyde (D5) and 5-nitrosalicylaldehyde (D6), it is found during the docking that residue G259 appears to exert a strong force on the D5 and D6 aldehyde groups, which is not available for other aldehydes during the docking. Besides,

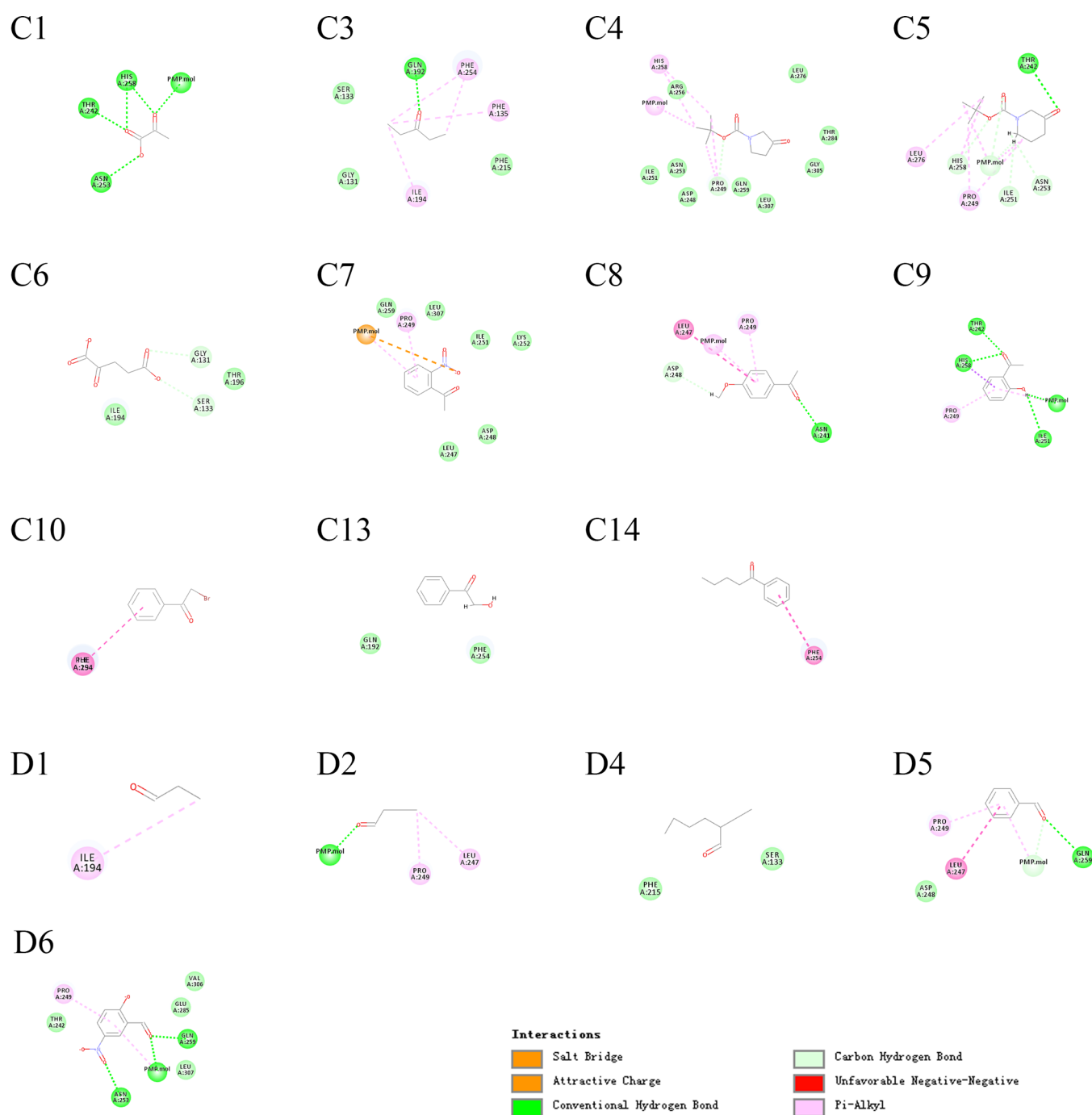


Figure 7. Docking results of *CbTA* with selected amino acceptors listed in Tables 3 and 4.

the nitro group of D6 appears to have an additional force on the active site as an electron-withdrawing group.

2.6. Site-Specific Mutagenesis of *CbTA*. The enzymatic transamination of ketones to amines is an important method to obtain various chiral building blocks or pharmaceuticals. In this study, a new ω -TA, *CbTA*, was obtained and its enzymatic properties and substrate spectrum were determined, showing the potential of *CbTA* for the production of chiral amines and unnatural amino acids. However, the unsatisfactory activity of *CbTA* on many ketones is a vital obstacle for its application in chiral amine production. In order to improve its activity, site-saturation mutagenesis was conducted on the basis of the previous results and homology modeling.

As confirmed by Voss et al., residues F130, Y190, Q190, G288, and A348 showed significant influence on the activity of amine transaminase. The docking result of *CbTA* with PLP and (*R*)-MBA indicated that residues K252, E285, G288, Q192, and Y190 are all located in the small pocket of the active site. Hereby, residues Y190, Q192, and G288 are selected for site-specific mutagenesis, and the results are presented in Figure 8. The results showed that the changes in residues Y190 and Q192 did have a significant effect on the activity of *CbTA* to (*R*)-MBA. Among them, mutant Q192G was the most beneficial mutation. The activity of the mutant Q192G is 9.8 times than that of the parental enzyme. However, there was no significant change in the activity of mutants G288 for *CbTA*.

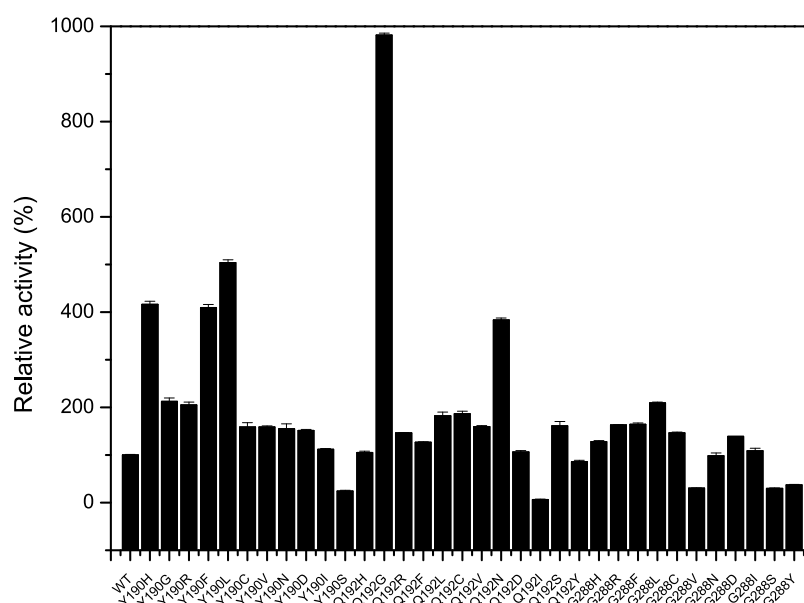


Figure 8. Results of site-specific mutagenesis of *CbTA*.

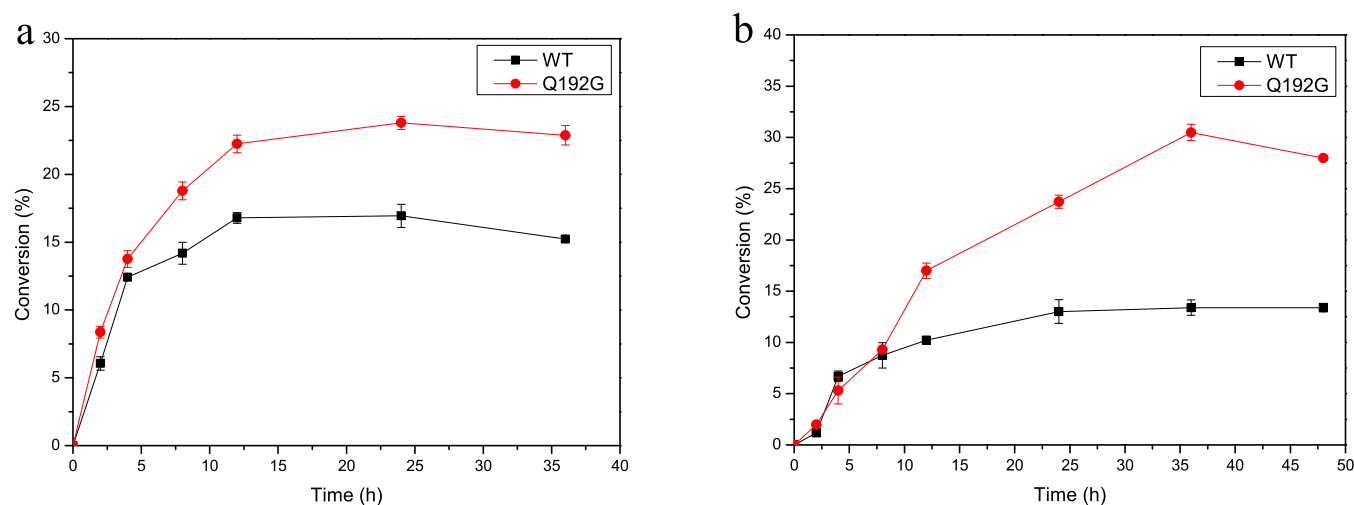


Figure 9. Conversion of *N*-Boc-3-pyrrolidinone and *N*-Boc-3-piperidone by the ω -TA and its Q192G mutant: (a) *N*-Boc-3-pyrrolidinone and (b) *N*-Boc-3-piperidone. Reaction conditions: 0.1 mg mL⁻¹ purified enzyme, 25 mM D-Ala, 25 mM of either *N*-Boc-pyrrolidinone or *N*-Boc-piperidone, 0.02 mM PLP, 1 mL of glycine–NaOH buffer (50 mM, pH 8.5), and 45 °C.

Chiral *N*-heterocyclic molecules, especially compounds with amino groups, such as 3-aminopiperidines, are valuable intermediates in the production of biologically active compounds with pharmacological properties.⁴⁶ Subsequently, *CbTA* and mutant Q192G are further applied to evaluate the conversion of cyclic substrates with a ketone group, and the results are shown in Figure 9. After 36 h of reaction, the conversion of *N*-Boc-pyrrolidinone and *N*-Boc-piperidone by *CbTA* was about 15% and 12%, and the conversion of *N*-Boc-pyrrolidinone and *N*-Boc-piperidone by mutant Q192G was increased to 23% and 30%, respectively. Compared with the parental *CbTA*, the reactivity of the mutant Q192G to cyclic substrates was obviously improved.

3. MATERIALS AND METHODS

3.1. Reagents. All the chemicals used were of analytical grade and purchased from Shanghai Aladdin Biochemical

Technology Co. Ltd. or Sigma-Aldrich, Inc. unless otherwise noted.

3.2. Sequence Analysis. The Ata-117 Armut11 sequences from *Arthrobacter sp.* KNK168 and amine transaminase from *A. terreus* NIH2624 were used as templates for BLAST search in NCBI to find new ω -TA sequences. After removing incomplete and redundant sequences, MEGA 7.0 was used to align all the unknown sequences in the identity range of 20–60% toward the templates, and the target sequences that conform to the functional characteristics of (*R*)-selective ω -TA with conserved sites R86, K188, and E221 were screened out according to the motif sequence [31 H/R****Y*V/*S(T/A/H/P), 95 F(Y)-VE(ANQ)] as confirmed in ref 14. Among them, a putative (*R*)-selective ω -TA from *C. bacterium* (*CbTA*) was chosen for further study, which shows 38% identity with Ata-117 Armut11. A phylogenetic tree was also generated with MEGA 7.0 by using the neighbor-joining algorithm.^{47,48}

Table 5. List of Primer Sequences for the Creation of *CbTA* Variants

primer name	5' → 3' nucleotide sequence	primer name	5' → 3' nucleotide sequence
Y190R F	GAT GCG CGT GTT CAG GTG ATC GTT ACC CGT	Q192Y F	TAC GTT TAT GTG ATC GTT ACC CGT GGT CTG
Y190R R	CTG AAC ACG CGC ATC ACG GTG ACC CGC ACG	Q192Y R	GAT CAC ATA AAC GTA CGC ATC ACG GTG ACC
Y190F F	GAT GCG TTT GTT CAG GTG ATC GTT ACC CGT	Q192H F	TAC GTT CAT GTG ATC GTT ACC CGT GGT CTG
Y190F R	CTG AAC AAA CGC ATC ACG GTG ACC CGC ACG	Q192H R	GAT CAC ATG AAC GTA CGC ATC ACG GTG ACC
Y190L F	GAT GCG CTT GTT CAG GTG ATC GTT ACC CGT	Q192N F	TAC GTT AAT GTG ATC GTT ACC CGT GGT CTG
Y190L R	CTG AAC AAG CGC ATC ACG GTG ACC CGC ACG	Q192N R	GAT CAC ATT AAC GTA CGC ATC ACG GTG ACC
Y190I F	GAT GCG ATT GTT CAG GTG ATC GTT ACC CGT	Q192D F	TAC GTT GAT GTG ATC GTT ACC CGT GGT CTG
Y190I R	CTG AAC AAT CGC ATC ACG GTG ACC CGC ACG	Q192D R	GAT CAC ATC AAC GTA CGC ATC ACG GTG ACC
Y190V F	GAT GCG GTT GTT CAG GTG ATC GTT ACC CGT	Q192C F	TAC GTT TGT GTG ATC GTT ACC CGT GGT CTG
Y190V R	CTG AAC AAC CGC ATC ACG GTG ACC CGC ACG	Q192C R	GAT CAC ACA AAC GTA CGC ATC ACG GTG ACC
Y190S F	GAT GCG AGT GTT CAG GTG ATC GTT ACC CGT	Q192G F	TAC GTT GGT GTG ATC GTT ACC CGT GGT CTG
Y190S R	CTG AAC ACT CGC ATC ACG GTG ACC CGC ACG	Q192G R	GAT CAC ACC AAC GTA CGC ATC ACG GTG ACC
Y190H F	GAT GCG CAT GTT CAG GTG ATC GTT ACC CGT	G288R F	AGC CGT CGT GCG AAC GTG TTT CTG ATT CAA
Y190H R	CTG AAC ATG CGC ATC ACG GTG ACC CGC ACG	G288R R	GTT CGC ACG ACG GCT TTC GGT CAG GTA ACC
Y190N F	GAT GCG AAT GTT CAG GTG ATC GTT ACC CGT	G288F F	AGC CGT TTT GCG AAC GTG TTT CTG ATT CAA
Y190N R	CTG AAC ATT CGC ATC ACG GTG ACC CGC ACG	G288F R	GTT CGC AAA ACG GCT TTC GGT CAG GTA ACC
Y190D F	GAT GCG GAT GTT CAG GTG ATC GTT ACC CGT	G288L F	AGC CGT CTT GCG AAC GTG TTT CTG ATT CAA
Y190D R	CTG AAC ATC CGC ATC ACG GTG ACC CGC ACG	G288L R	GTT CGC AAG ACG GCT TTC GGT CAG GTA ACC
Y190C F	GAT GCG TGT GTT CAG GTG ATC GTT ACC CGT	G288I F	AGC CGT ATT GCG AAC GTG TTT CTG ATT CAA
Y190C R	CTG AAC ACA CGC ATC ACG GTG ACC CGC ACG	G288I R	GTT CGC AAT ACG GCT TTC GGT CAG GTA ACC
Y190G F	GAT GCG GGT GTT CAG GTG ATC GTT ACC CGT	G288V F	AGC CGT GTT GCG AAC GTG TTT CTG ATT CAA
Y190G R	CTG AAC ACC CGC ATC ACG GTG ACC CGC ACG	G288V R	GTT CGC AAC ACG GCT TTC GGT CAG GTA ACC
Q192R F	TAC GTT CGT GTG ATC GTT ACC CGT GGT CTG	G288S F	AGC CGT AGT GCG AAC GTG TTT CTG ATT CAA
Q192R R	GAT CAC ACG AAC GTA CGC ATC ACG GTG ACC	G288S R	GTT CGC ACT ACG GCT TTC GGT CAG GTA ACC
Q192F F	TAC GTT TTT GTG ATC GTT ACC CGT GGT CTG	G288Y F	AGC CGT TAT GCG AAC GTG TTT CTG ATT CAA
Q192F R	GAT CAC AAA AAC GTA CGC ATC ACG GTG ACC	G288Y R	GTT CGC ATA ACG GCT TTC GGT CAG GTA ACC
Q192L F	TAC GTT CTT GTG ATC GTT ACC CGT GGT CTG	G288H F	AGC CGT CAT GCG AAC GTG TTT CTG ATT CAA
Q192L R	GAT CAC AAG AAC GTA CGC ATC ACG GTG ACC	G288H R	GTT CGC ATG ACG GCT TTC GGT CAG GTA ACC
Q192I F	TAC GTT ATT GTG ATC GTT ACC CGT GGT CTG	G288N F	AGC CGT AAT GCG AAC GTG TTT CTG ATT CAA
Q192I R	GAT CAC AAT AAC GTA CGC ATC ACG GTG ACC	G288N R	GTT CGC ATT ACG GCT TTC GGT CAG GTA ACC
Q192V F	TAC GTT GTT GTG ATC GTT ACC CGT GGT CTG	G288D F	AGC CGT GAT GCG AAC GTG TTT CTG ATT CAA
Q192V R	GAT CAC AAC AAC GTA CGC ATC ACG GTG ACC	G288D R	GTT CGC ATC ACG GCT TTC GGT CAG GTA ACC
Q192S F	TAC GTT AGT GTG ATC GTT ACC CGT GGT CTG	G288C F	AGC CGT TGT GCG AAC GTG TTT CTG ATT CAA
Q192S R	GAT CAC ACT AAC GTA CGC ATC ACG GTG ACC	G288C R	GTT CGC ACA ACG GCT TTC GGT CAG GTA ACC

3.3. Plasmid and Strain Construction. The gene sequence of the putative *CbTA* was further codon-optimized and synthesized by GenScript (Nanjing, China). The encoding region was inserted between the BamH I and Xho I, with a 6-histidine tag at the *N*-terminal, resulting in plasmid pRSF-*CbTA*. The recombinant plasmid was transformed into *E. coli* BL21(DE3) to generate the recombinant strain of *E. coli* BL21(DE3)/pRSF-*CbTA*.

3.4. Expression and Purification of Recombinant *CbTA*. Recombinant *E. coli* BL21(DE3)/pRSF-*CbTA* was cultured in 100 mL of LB medium (1.0% peptone, 0.5% yeast extract, and 1.0% NaCl) with kanamycin (50 $\mu\text{g}/\text{mL}$) at 37 °C and 200 rpm. When the OD₆₀₀ of the culture reaches about 0.6, 0.02 mM isopropyl β -D-1-thiogalactopyranoside (IPTG) was added, and the culture was cultivated at 20 °C for another 24 h. Thereafter, the cells were harvested, re-suspended in 20 mL of glycine–NaOH buffer (50 mM, pH 8.5), and sonicated in an ice bath for 30 min. The cell debris were removed by centrifugation at 8000 $\times g$ at 4 °C for 40 min. The supernatant was passed through a 5 mL Ni-NTA column to purify recombinant *CbTA*, and then the purified *CbTA* solution was stored at 4 °C for further experiments. The molecular weight of the purified *CbTA* was determined by 12% (w/v) SDS-PAGE.⁴⁹ A control experiment was performed under the same conditions using an *E. coli* transformant carrying empty pRSFDuet-1.

3.5. Characterization of Biochemical Properties. By using the following buffers with different pH values of 6.0–10.5, 50 mM phosphate buffer, pH 6.0–8.0, and 50 mM glycine–NaOH buffer, pH 8.5–10.5, the optimal pH of *CbTA* was determined at 40 °C. The optimal temperature for *CbTA* was investigated from 25 to 65 °C at pH 8.5. Relative activity (%) was calculated using the maximal activity as a control (100%). The temperature stability was measured by incubating *CbTA* for a period in the temperature range of 40–65 °C.

The tolerance of *CbTA* to organic solvents is determined by incubating 100 μL of *CbTA* in glycine–NaOH buffer (50 mM, pH 8.5) for 5 h at room temperature. The buffer contains 0, 5, 10, 20, 40, 60, and 80% (v/v) organic cosolvents (acetonitrile or DMSO or methanol or ethanol). After that, residual activities were evaluated using the assay method of enzyme activity described below.

3.6. Assay of Enzyme Activity. Enzyme activity analysis was performed in 500 μL of glycine–NaOH buffer (50 mM, pH 8.5) containing PLP (20 μM), (*R*)-MBA (10 mM), and sodium pyruvate (10 mM). The reaction started at 45 °C by adding 0.05 mg of the purified *CbTA* to the mixture. After 30 min, the mixture was heated and boiled for 20 min to stop the reaction. All the experiments were performed in triplicate. The resulting acetophenone was analyzed by high-performance liquid

chromatography (HPLC). One unit of enzyme activity was defined as the production of 1 μmol acetophenone per minute.

3.7. Determination of Kinetic Parameters. The kinetic parameters of *CbTA* to (*R*)-MBA or pyruvate were measured at 45 °C and pH 8.5. According to the method described above, the initial reaction rate was determined under the conditions of different concentrations of (*R*)-MBA or pyruvate. The production of acetophenone and the consumption of pyruvate were analyzed by HPLC. In order to determine the kinetic parameters of *CbTA* to (*R*)-MBA, the reaction solution was 500 μL of glycine–NaOH buffer (50 mM, pH 8.5) containing 20 mM pyruvate, 0.05 mg of *CbTA*, 0.02 mM PLP, and different concentrations of (*R*)-MBA. The kinetic parameters of *CbTA* to pyruvate was measured in 500 μL of glycine–NaOH buffer (50 mM, pH 8.5) containing 20 mM (*R*)-MBA, 0.05 mg of *CbTA*, 0.02 mM PLP, and different concentrations of sodium pyruvate. The K_m and k_{cat} values of (*R*)-MBA and pyruvate were calculated according to the nonlinear regression fitting of the Michaelis–Menten equation.

3.8. Characterization of the Substrate Specificity of *CbTA*. Substrate specificity of *CbTA* was tested by reactions between different groups of amino donors and amino receptors. All the experiments were performed in triplicate. When the specificity of amino donors is studied, amino donors used are listed in Tables 1, 2. The activity assay for each reaction was carried out in a 50 mM glycine–NaOH buffer (pH 8.5) containing 25 mM amino donor, 25 mM sodium pyruvate, 0.02 mM PLP, and a suitable amount of purified *CbTA*, with a final volume of 500 μL at 40 °C for 30 min. The activity of *CbTA* against different amino receptors was compared by measuring the amount of acetophenone produced. When the specificity of amino receptors is studied, amino receptors used are listed in Tables 3, 4. The activity assay for each reaction was carried out in a 50 mM glycine–NaOH buffer (pH 8.5) containing 25 mM (*R*)-MBA, 25 mM amino receptor, 0.02 mM PLP, and a suitable amount of purified *CbTA*, with a final volume of 500 μL at 40 °C for 30 min. The activity of *CbTA* against different amino donors was compared by measuring the reduction in pyruvate.

3.9. Molecular Modeling and Substrate Docking. Molecular modeling was performed using Modeller 9.24 and I-Tasser (<https://zhanglab.ccmb.med.umich.edu/I-Tasser/>). The homology model was based on the crystal structure (PDB: 3WWH,²³ 4CE5,²⁴ 4CMD,²⁷ 4UUG,²⁵ and SE25²⁶), and the best model was selected by Ramachandran analysis.

3.10. Site-Specific Mutagenesis. The amino acid residues Y190, Q192, and G288 were selected for site-specific mutagenesis on the basis of the previous results and modeling analysis.¹⁹ The site-specific mutagenesis was designed by a NDT codon design. All primers are listed in Table 5. Site-specific mutagenesis was performed according to the instructions of a site-directed mutagenesis kit (MutExpress II Fast Mutagenesis Kit V2, Vazyme, Nanjing, China). Mutations were introduced by the mutagenesis polymerase chain reaction. The amplified fragments were digested with DpnI at 37 °C for 1 h, and the recombinant plasmid was transformed into *E. coli* BL21(DE3) for screening. Individual colonies of the transformants were transferred to 96-well plates containing 300 μL of LB medium with kanamycin (50 $\mu\text{g}/\text{mL}$), 96-well plates were incubated overnight (37 °C, 200 rpm). Subsequently, 30 μL of that culture suspension was transferred to a medium containing 300 μL of fresh LB in each well for culture for 2 h (37 °C, 200 rpm), and then 300 μL of LB containing 0.04 mM IPTG was added and induced at 20 °C for 24 h and the sludge was collected by

centrifugation at 4200 rpm for 20 min. The cells were fragmented according to a fragmentation kit (xTractor Buffer Kit, TAKARA, Japan). After the cells were allowed to stand at room temperature for 30 min, the crude mutant *CbTA* solution was collected by centrifugation. Thereafter, the activity of the mutants was tested as described above.

3.11. HPLC Analysis. The acetophenone was measured at 254 nm by HPLC (Agilent 1260) using an Agilent C18 column (250 mm \times 4.6 mm) at 30 °C.⁴¹ The mobile phase is water/acetonitrile (50:50, v/v) and the flow rate is 1 mL/min.

The pyruvate was measured at 210 nm by HPLC (Agilent 1260) using an Agilent C18 column (250 mm \times 4.6 mm) at 30 °C. The mobile phase is methyl alcohol/water/phosphoric acid (20:80:0.03, v/v) and the flow rate is 0.8 mL/min.

The chiral MBA were detected by HPLC (Agilent 1260) with a CR-I(+) chiral column (150 mm \times 3.0 mm) (Daicel Corp.) at 254 nm and 30 °C. The eluent is water/acetonitrile (70:30, v/v) containing 0.36% trifluoroacetic acid at a flow rate of 0.4 mL/min.

The analyses of *N*-Boc-3-pyrrolidinone, *N*-Boc-3-piperidone, *N*-Boc-3-aminopyrrolidine, and *N*-Boc-3-aminopiperidine were performed on a HPLC system (Agilent 1260) with an Agilent C18 column (250 mm \times 4.6 mm) at 220 nm and 25 °C. Elution was carried out with a mobile phase of water/acetonitrile/diethanolamine (70:30:0.1, v/v/v) at a rate of 1 mL/min.⁴⁶

4. CONCLUSIONS

(*R*)-selective ω -TAs has great potential for industrial applications. In this work, *CbTA*, a hypothetical (*R*)-selective ω -TA from *C. bacterium* was found by the motif sequence BLAST from genome mining. On the basis of the amino acid sequences, a phylogenetic tree was constructed to verify the taxonomic and evolutionary relationships of *CbTA* with other amine transaminase family homologues. Nine amino acid sequences with different degrees of sequence identity to *CbTA* were selected and analyzed, and *CbTA* showed a close evolutionary relationship to pyruvate transferase from *M. vanbaalenii* PYR-1 and Ata-117 Arrmut11. By characterizing the enzymatic properties of *CbTA*, results showed that *CbTA* has good thermal stability, organic solvent tolerance, and broad substrate specificity. Thereafter, the site-specific mutagenesis of *CbTA* was conducted and the mutant Q192G with higher activity was screened, which was applied in conversions of *N*-Boc-pyrrolidinone and *N*-Boc-piperidone. The results showed that *CbTA* can be used as a valuable catalyst for the asymmetric synthesis of chiral amines from the corresponding aldehydes or ketones.

AUTHOR INFORMATION

Corresponding Authors

Honghua Jia – College of Biotechnology and Pharmaceutical Engineering, Nanjing Tech University, Nanjing 211816, China; orcid.org/0000-0002-3824-7768; Email: [hhjia@njtech.edu.cn](mailto:hjhjia@njtech.edu.cn)

Yan Li – College of Biotechnology and Pharmaceutical Engineering, Nanjing Tech University, Nanjing 211816, China; Email: liyan@njtech.edu.cn

Authors

Chen Wang – College of Biotechnology and Pharmaceutical Engineering, Nanjing Tech University, Nanjing 211816, China

Kexin Tang – College of Biotechnology and Pharmaceutical Engineering, Nanjing Tech University, Nanjing 211816, China

Ya Dai – College of Biotechnology and Pharmaceutical Engineering, Nanjing Tech University, Nanjing 211816, China

Zhen Gao – College of Biotechnology and Pharmaceutical Engineering, Nanjing Tech University, Nanjing 211816, China

Bin Wu – College of Biotechnology and Pharmaceutical Engineering, Nanjing Tech University, Nanjing 211816, China;  orcid.org/0000-0003-3785-1266

Complete contact information is available at:
<https://pubs.acs.org/10.1021/acsomega.1c02164>

Author Contributions

C.W. conducted most of the experiments and drafted the manuscript. K.T. and Y.D. performed some experiments. Y.L. and H.J. designed and supervised the project. Z.G. and B.W. discussed the design and results. All the authors commented and approved the manuscript.

Notes

The authors declare no competing financial interest.

ACKNOWLEDGMENTS

We acknowledge the financial support from Jiangsu Agricultural Science and Technology Innovation Fund Project (CX(19)2001), Qing Lan Project of Jiangsu Universities, Six Talent Peaks Project in Jiangsu Province, the Jiangsu Synergetic Innovation Center for Advanced Bio-manufacture, and PAPD.

ABBREVIATIONS

PLP	pyridoxal 5'-phosphate
PMP	pyridoxamine 5'-phosphate
D-Ala	D-alanine
(R)-MBA	(R)-methylbenzylamine
ω -TA	ω -transaminase
HPLC	high-performance liquid chromatography
IPTG	isopropyl β -D-1-thiogalactopyranoside
PCR	polymerase chain reaction
SDS-PAGE	sodium dodecyl sulfate polyacrylamide gel electrophoresis
ee	enantiomeric excess

REFERENCES

- (1) Rehn, G.; Adlercreutz, P.; Grey, C. Supported liquid membrane as a novel tool for driving the equilibrium of ω -transaminase catalyzed asymmetric synthesis. *J. Biotechnol.* **2014**, *179*, 50–55.
- (2) Fuchs, M.; Farnberger, J. E.; Kroutil, W. The industrial age of biocatalytic transamination. *Eur. J. Org. Chem.* **2015**, 6965–6982.
- (3) Schrittwieser, J. H.; Velikogne, S.; Hall, M.; Kroutil, W. Artificial biocatalytic linear cascades for preparation of organic molecules. *Chem. Rev.* **2018**, *118*, 270–348.
- (4) Kroutil, W.; Fischereider, E.-M.; Fuchs, C. S.; Lechner, H.; Mutti, F. G.; Pressnitz, D.; Rajagopalan, A.; Sattler, J. H.; Simon, R. C.; Siirola, E. Asymmetric preparation of prim-, sec-, and tert- amines employing selected biocatalysts. *Org. Process Res. Dev.* **2013**, *17*, 751–759.
- (5) Kohls, H.; Steffen-Munsberg, F.; Höhne, M. Recent achievements in developing the biocatalytic toolbox for chiral amine synthesis. *Curr. Opin. Chem. Biol.* **2014**, *19*, 180–192.
- (6) Han, S.-W.; Shin, J.-S. Kinetic analysis of R-selective ω -transaminases for determination of intrinsic kinetic parameters and computational modeling of kinetic resolution of chiral amine. *Appl. Biochem. Biotechnol.* **2020**, *191*, 92–103.

(7) Guo, F.; Berglund, P. Transaminase biocatalysis: optimization and application. *Green Chem.* **2017**, *19*, 333–360.

(8) Kara, S.; Schrittwieser, J. H.; Hollmann, F.; Ansorge-Schumacher, M. B. Recent trends and novel concepts in cofactor-dependent biotransformations. *Appl. Microbiol. Biotechnol.* **2014**, *98*, 1517–1529.

(9) Koszelewski, D.; Tauber, K.; Faber, K.; Kroutil, W. ω -Transaminases for the synthesis of non-racemic α -chiral primary amines. *Trends Biotechnol.* **2010**, *28*, 324–332.

(10) Savile, C. K.; Janey, J. M.; Mundorff, E. C.; Moore, J. C.; Tam, S.; Jarvis, W. R.; Colbeck, J. C.; Krebber, A.; Fleitz, F. J.; Brands, J.; Devine, P. N.; Huisman, G. W.; Hughes, G. J. Biocatalytic asymmetric synthesis of chiral amines from ketones applied to sitagliptin manufacture. *Science* **2010**, *329*, 305–309.

(11) Park, E.-S.; Kim, M.; Shin, J.-S. Molecular determinants for substrate selectivity of ω -transaminases. *Appl. Microbiol. Biotechnol.* **2012**, *93*, 2425–2435.

(12) Malik, M. S.; Park, E.-S.; Shin, J.-S. Features and technical applications of ω -transaminases. *Appl. Microbiol. Biotechnol.* **2012**, *94*, 1163–1171.

(13) Höhne, M.; Bornscheuer, U. T. Biocatalytic routes to optically active amines. *ChemCatChem* **2009**, *1*, 42–51.

(14) Höhne, M.; Schätzle, S.; Jochens, H.; Robins, K.; Bornscheuer, U. T. Rational assignment of key motifs for function guides in silico enzyme identification. *Nat. Chem. Biol.* **2010**, *6*, 807–813.

(15) Jiang, J.; Chen, X.; Zhang, D.; Wu, Q.; Zhu, D. Characterization of (R)-selective amine transaminases identified by in silico motif sequence blast. *Appl. Microbiol. Biotechnol.* **2014**, *99*, 2613–2621.

(16) Zeifman, Y. S.; Boyko, K. M.; Nikolaeva, A. Y.; Timofeev, V. I.; Rakitina, T. V.; Popov, V. O.; Bezsudnova, E. Y. Functional characterization of PLP fold type IV transaminase with a mixed type of activity from *Haliangium ochraceum*. *Biochim. Biophys. Acta, Proteins Proteomics* **2019**, *1867*, 575–585.

(17) Bezsudnova, E. Y.; Dibrova, D. V.; Nikolaeva, A. Y.; Rakitina, T. V.; Popov, V. O. Identification of branched-chain amino acid aminotransferases active towards (R)-(+)-1-phenylethylamine among PLP fold type IV transaminases. *J. Biotechnol.* **2018**, *271*, 26–28.

(18) Skalden, L.; Thomsen, M.; Höhne, M.; Bornscheuer, U. T.; Hinrichs, W. Structural and biochemical characterization of the dual substrate recognition of the (R)-selective amine transaminase from *Aspergillus fumigatus*. *FEBS J.* **2015**, *282*, 407–415.

(19) Voss, M.; Xiang, C.; Esque, J.; Nobili, A.; Menke, M. J.; André, I.; Höhne, M.; Bornscheuer, U. T. Creation of (R)-amine transaminase activity within an α -amino acid transaminase scaffold. *ACS Chem. Biol.* **2020**, *15*, 416–424.

(20) Cheng, F.; Chen, X.-L.; Xiang, C.; Liu, Z.-Q.; Wang, Y.-J.; Zheng, Y.-G. Fluorescence-based high-throughput screening system for R- ω -transaminase engineering and its substrate scope extension. *Appl. Microbiol. Biotechnol.* **2020**, *104*, 2999–3009.

(21) Cheng, F.; Chen, X.-L.; Li, M.-Y.; Zhang, X.-J.; Jia, D.-X.; Wang, Y.-J.; Liu, Z.-Q.; Zheng, Y.-G. Creation of a robust and R-selective ω -amine transaminase for the asymmetric synthesis of sitagliptin intermediate on a kilogram scale. *Enzyme Microb. Technol.* **2020**, *141*, 109655.

(22) Cuetos, A.; García-Ramos, M.; Fischereider, E.-M.; Díaz-Rodríguez, A.; Grogan, G.; Gotor, V.; Kroutil, W.; Lavandera, I. Catalytic promiscuity of transaminases: Preparation of enantioenriched β -fluoroamines by formal tandem hydrodefluorination/deamination. *Angew. Chem., Int. Ed.* **2016**, *55*, 3144.

(23) Guan, L.-J.; Ohtsuka, J.; Okai, M.; Miyakawa, T.; Mase, T.; Zhi, Y.; Hou, F.; Ito, N.; Iwasaki, A.; Yasohara, Y.; Tanokura, M. A new target region for changing the substrate specificity of amine transaminases. *Sci. Rep.* **2015**, *5*, 10753.

(24) Łyskowski, A.; Gruber, C.; Steinkellner, G.; Schürmann, M.; Schwab, H.; Gruber, K.; Steiner, K. Crystal structure of an (R)-selective ω -transaminase from *Aspergillus terreus*. *PLoS One* **2014**, *9*, No. e87350.

(25) Hu, Y.; Jia, X.; Lu, Z.; Han, L. Characterization of crystal structure and key residues of *Aspergillus fumigatus* nucleoside diphosphate kinase. *Biochem. Biophys. Res. Commun.* **2019**, *511*, 148–153.

- (26) Isupov, M. N.; Boyko, K. M.; Sutter, J.-M.; James, P.; Sayer, C.; Schmidt, M.; Schönheit, P.; Nikolaeva, A. Y.; Stekhanova, T. N.; Mardanov, A. V.; Ravin, N. V.; Bezsudnova, E. Y.; Popov, V. O.; Littlechild, J. A. Thermostable branched-chain amino acid transaminases from the archaea *Geoglobus acetivorans* and *Archaeoglobus fulgidus*: Biochemical and structural characterization. *Front. Bioeng. Biotechnol.* **2019**, *7*, 7.
- (27) Sayer, C.; Martinez-Torres, R. J.; Richter, N.; Isupov, M. N.; Hales, H. C.; Littlechild, J. A.; Ward, J. M. The substrate specificity, enantioselectivity and structure of the (R)-selective amine: pyruvate transaminase from *Nectria haematococca*. *FEBS J.* **2014**, *281*, 2240.
- (28) Shin, J.-S.; Kim, B.-G. Comparison of the ω -transaminases from different microorganisms and application to production of chiral amines. *Biosci., Biotechnol., Biochem.* **2001**, *65*, 1782–1788.
- (29) Steffen-Munzberg, F.; Vickers, C.; Thontowi, A.; Schätzle, S.; Meinhardt, T.; Svedendahl Humble, M.; Land, H.; Berglund, P.; Bornscheuer, U. T.; Höhne, M. Revealing the structural basis of promiscuous amine transaminase activity. *ChemCatChem* **2013**, *5*, 154–157.
- (30) Iwasaki, A.; Matsumoto, K.; Hasegawa, J.; Yasohara, Y. A novel transaminase, (R)-amine:pyruvate aminotransferase, from *Arthrobacter* sp. KNK168 (FERM BP-5228): purification, characterization, and gene cloning. *Appl. Microbiol. Biotechnol.* **2012**, *93*, 1563–1573.
- (31) Boyko, K. M.; Stekhanova, T. N.; Nikolaeva, A. Y.; Mardanov, A. V.; Rakitin, A. L.; Ravin, N. V.; Bezsudnova, E. Y.; Popov, V. O. First structure of archaeal branched-chain amino acid aminotransferase from *Thermoproteus uzoniensis* specific for L-amino acids and R-amines. *Extremophiles* **2016**, *20*, 215–225.
- (32) Bruins, M. E.; Janssen, A. E. M.; Boom, R. M. Thermozyms and their applications: A review of recent literature and patents. *Appl. Biochem. Biotechnol.* **2001**, *90*, 155–186.
- (33) Chen, Y.; Yi, D.; Jiang, S.; Wei, D. Identification of novel thermostable taurine-pyruvate transaminase from *Geobacillus thermodenitrificans* for chiral amine synthesis. *Appl. Microbiol. Biotechnol.* **2016**, *100*, 3101–3111.
- (34) Atalah, J.; Cáceres-Moreno, P.; Espina, G.; Blamey, J. M. Thermophiles and the applications of their enzymes as new biocatalysts. *Bioresour. Technol.* **2019**, *280*, 478–488.
- (35) Mathew, S.; Deepankumar, K.; Shin, G.; Hong, E. Y.; Kim, B.-G.; Chung, T.; Yun, H. Identification of novel thermostable ω -transaminase and its application for enzymatic synthesis of chiral amines at high temperature. *RSC Adv.* **2016**, *6*, 69257–69260.
- (36) Ferrandi, E. E.; Bassanini, I.; Sechi, B.; Vanoni, M.; Tessaro, D.; Guðbergssdóttir, S. R.; Riva, S.; Peng, X.; Monti, D. Discovery and characterization of a novel thermostable β -amino acid transaminase from a *Meiothermus* strain isolated in an Icelandic hot spring. *Biotechnol. J.* **2020**, *15*, 2000125.
- (37) Ferrandi, E. E.; Previdi, A.; Bassanini, I.; Riva, S.; Peng, X.; Monti, D. Novel thermostable amine transferases from hot spring metagenomes. *Appl. Microbiol. Biotechnol.* **2017**, *101*, 4963–4979.
- (38) Kelly, S. A.; Magill, D. J.; Megaw, J.; Skvortsov, T.; Allers, T.; McGrath, J. W.; Allen, C. C. R.; Moody, T. S.; Gilmore, B. F. Characterisation of a solvent-tolerant haloarchaeal (R)-selective transaminase isolated from a Triassic Period salt mine. *Appl. Microbiol. Biotechnol.* **2019**, *103*, 5727–5737.
- (39) Gao, S.; Su, Y.; Zhao, L.; Li, G.; Zheng, G. Characterization of a (R)-selective amine transaminase from *Fusarium oxysporum*. *Process Biochem.* **2017**, *63*, 130–136.
- (40) Pavlidis, I. V.; Weiß, M. S.; Genz, M.; Spurr, P.; Hanlon, S. P.; Wirz, B.; Iding, H.; Bornscheuer, U. T. Identification of (S)-selective transaminases for the asymmetric synthesis of bulky chiral amines. *Nat. Chem.* **2016**, *8*, 1076–1082.
- (41) Shin, J.-S.; Kim, B.-G. Exploring the active site of amine:pyruvate aminotransferase on the basis of the substrate structure–reactivity relationship: How the enzyme controls substrate specificity and stereoselectivity. *J. Org. Chem.* **2002**, *67*, 2848–2853.
- (42) Iglesias, C.; Panizza, P.; Rodriguez Giordano, S. Identification, expression and characterization of an R- ω -transaminase from *Capronia semiimmersa*. *Appl. Microbiol. Biotechnol.* **2017**, *101*, 5677–5687.
- (43) Jiang, J.; Chen, X.; Feng, J.; Wu, Q.; Zhu, D. Substrate profile of an ω -transaminase from *Burkholderia vietnamiensis* and its potential for the production of optically pure amines and unnatural amino acids. *J. Mol. Catal. B: Enzym.* **2014**, *100*, 32–39.
- (44) Eliot, A. C.; Kirsch, J. F. Pyridoxal phosphate enzymes: mechanistic, structural, and evolutionary considerations. *Annu. Rev. Biochem.* **2004**, *73*, 383–415.
- (45) Skalden, L.; Thomsen, M.; Höhne, M.; Bornscheuer, U. T.; Hinrichs, W. Structural and biochemical characterization of the dual substrate recognition of the (R)-selective amine transaminase from *Aspergillus fumigatus*. *FEBS J.* **2014**, *282*, 407–415.
- (46) Petri, A.; Colonna, V.; Piccolo, O. Asymmetric synthesis of a high added value chiral amine using immobilized ω -transaminases. *Beilstein J. Org. Chem.* **2019**, *15*, 60–66.
- (47) Kumar, S.; Stecher, G.; Tamura, K. MEGA7: Molecular evolutionary genetics analysis version 7.0 for bigger datasets. *Mol. Biol. Evol.* **2016**, *33*, 1870–1874.
- (48) Saitou, N.; Nei, M. The neighbor-joining method: a new method for reconstructing phylogenetic trees. *Mol. Biol. Evol.* **1987**, *4*, 406–425.
- (49) Schägger, H.; von Jagow, G. Tricine-sodium dodecyl sulfate-polyacrylamide gel electrophoresis for the separation of proteins in the range from 1 to 100 kDa. *Anal. Biochem.* **1987**, *166*, 368–379.